STAT5b is a marker of poor prognosis, rather than a therapeutic target in glioblastomas

NADÈGE DUBOIS[1,2], SHARON BERENDSEN[1], KATHERINE TAN[1], LAURENT SCHOYSMANS[3], WIM SPLIET[4], TATJANA SEUTE[1], VINCENT BOURS[2] and PIERRE A. ROBE[1,2]

[1]Department of Neurology and Neurosurgery, and The T&P Bohnenn Laboratory for Neuro-Oncology, University Medical Center of Utrecht, 3584CX Utrecht, The Netherlands; [2]Human Genetics Laboratory, GIGA-Cancer Center, University of Liège; [3]Department of Radiology, University Medical Center of Liège, 4000 Liege, Belgium; [4]Department of Pathology, University Medical Center of Utrecht, 3584CX Utrecht, The Netherlands

Received February 14, 2022; Accepted June 8, 2022

DOI: 10.3892/ijo.2022.5414

Abstract. The copy number and mRNA expression of STAT5b were assessed in samples from the TCGA repository of glioblastomas (GBM). The activation of this transcription factor was analyzed on tissue microarrays comprising 392 WHO 2016 GBM samples from our clinical practice. These data were correlated with patient survival using multivariable Cox analysis and, for a subset of 167 tumors, with signs of tumor invasiveness on the MRI. The effects of STAT5b knockdown by siRNA were assessed on the growth, therapeutic resistance, invasion and migration of GBM cell lines U87, U87-EGFRVIII and LN18 and primary cultures GM2 and GM3. The activation, but not the copy number or the mRNA expression of nuclear transcription factor STAT5b expression correlated inversely with patient survival independently of IDH1R132H status, age, Karnofsky Performance Score, treatment and tumor volume. STAT5b inhibition neither altered the cell proliferation nor reduced the clonogenic proliferative potency of GBM cells, and did not sensitize them to the cytotoxic effect of ionizing radiation and temozolomide *in vitro*. STAT5b inhibition significantly increased GBM cell migration, but decreased the invasion of some GBM cells *in vitro*. There was no correlation between the activation of STAT5b in clinical tumors and the extent of invasion on MRI OF patients. In conclusion, STAT5b is frequently activated in GBM and correlates inversely with patient survival. It does not contribute to the growth and resistance of these tumors, and is thus rather a potential prognostic marker than a therapeutic target in these tumors.

Correspondence to: Professor Pierre A. Robe, Department of Neurology and Neurosurgery, and The T&P Bohnenn Laboratory for Neuro-Oncology, University Medical Center of Utrecht, 100 Heidelberglaan Road, 3584CX Utrecht, The Netherlands
E-mail: p.robe@umcutrecht.nl

Key words: glioblastoma, STAT5b, patient survival, invasiveness, treatment resistance

Introduction

Glioblastomas (GBM), the most common primary brain tumors, carry a dismal prognosis despite aggressive surgery, chemotherapy and radiation therapy (1,2). Subsets of GBMs, defined by the activation of given signaling pathways (for instance, c-Met) or distinct driver genetic changes (for instance, IDH1/2 mutation), however present diverse outcomes (3,4). Novel therapeutic targets and solid markers of prognosis are thus of crucial importance in the fight against these types of cancer.

STAT5 transcription factors are composed of homologous protein dimers of either STAT5a or STAT5b, encoded by two different genes, and that show both overlapping and distinct regulation, transcriptional targets and biological effects (5). By modulating the expression of effectors such as Bcl-XL, Aurora A, FAK or VEGF, STAT5 was reported to contribute to GBM growth, invasion and therapeutic resistance (6-9). The transcriptional targets of STAT5a and b present certain overlap but are also differentiated (10). In malignant gliomas, STAT5a was revealed to be activated downstream of $EGFR_{VIII}$ (11) and to promote cell migration, survival and proliferation, notably via induction of the long non-coding RNA LINC01198 (12,13). Similarly, STAT5b is highly expressed and predominantly activated in these tumors (6,7), notably as a result of mir-134 repression (14) and high tyrosine kinase activity (11,15). A single nucleotide polymorphism of STAT5b was reported to associate with the risk of GBM (16), and STAT5b can associate with $EGFR_{VIII}$ in the nucleus in GBM that harbor this mutation, which activates the transcription of Bcl-XL. STAT5b was also reported to contribute to GBM cell proliferation (7). Univariable analysis in small series of glioma patients suggested an inverse correlation between STAT5b activation and patient survival (6,8,17). It was also found that epileptogenicity in GBM associates with an improved survival and with

a decreased HIF-STAT5b activation (18). As a result, STAT5b has been proposed as a potential target for the treatment of patients with GBM (16). The nature and the specificity of the tumorigenic role of STAT5b in GBM however varies between these reports, and its clinical value as a marker of survival or a therapeutic target still needs to be confirmed in large series of patients.

Therefore, the prognostic value of STAT5b expression in a large institutional cohort of 392 GBM samples and its association with tumor invasion on the MRIs of 167 of these tumors were analyzed. The effect of STAT5b inhibition on the proliferative, therapeutic resistance and migratory capacities of cultures of human GBM was further evaluated.

Materials and methods

Genetic analysis. The GISTIC 2.0 copy number data and Agilent-based mRNA expression data of 538 and 552 GBM samples respectively of the The Cancer Genome Atlas (TCGA) repository were obtained from the UCSC Cancer Genomics Browser (accessed in September 2015). Threshold copy number (CN) values were used to perform the correlations with mRNA expression data using Pearson's correlation analyses.

Ethics statement. The present study was conducted following review by the ethics committee of University Medical Center of Utrecht (Utrecht, The Netherlands) and the institutional review board (IRB; TC-Bio; approval no. 16-229). According to Dutch regulations, the need for informed consent was waived for this retrospective analysis of patient clinical data.

Tissue microarrays (TMAs), immunohistochemistry (IHC) and MR assessment. Formalin-fixed, paraffin-embedded tumor tissues of a series of 392 GBM (320 IDH 1 R132 wild-type, 18 IDH1 R132 mutant and 54 IDH1 status unknown) and 10 non-tumoral epileptic brains operated between 2005 and 2013 at the University Hospital Center of Utrecht were included in TMAs. Details on TMA construction and IHC have been previously described (19). The WHO 2016 classification was used to define and characterize these tumors. Primary antibodies to Phospho-STAT5b were used for the immunostaining, as previously described (20) and revealed using secondary antibodies and diaminobenzidine (DAB). Briefly, the 4-μm sectioned TMA slides, were deparaffinized in xylene and rehydrated with graded alcohol solutions. After peroxidase blocking with hydrogen peroxide (3%), antigen retrieval was achieved by incubation in citrate buffer (pH 6) for 12 min at 126˚C, blocked for 10 min at room temperature in Dako Protein Block Serum X090930-2 according to the manufacturer's protocol (Dako; Agilent Technologies, Inc.), and incubated with 731SP-Stat5b (1/50; cat. no. ab52211; Abcam) for 1 h at room temperature, and revealed with the EnvVision + System HRP (Dako; Agilent Technologies, Inc.) according to the manufacturer's protocol. The processed TMZ slides were scanned at high resolution on a Hamamatsu NDP scanner and visualized using the Hamamatsu NDP.view2 software for Mac OS (Hamamatsu Photonics K.K.). Protein expression evaluation was blinded to the clinical data and scored as negative (0% of cells with Phospho-STAT5b staining) or positive (>0% of cells with Phospho-STAT5b staining; IHC score 1 with 0-25% of cells with Phospho-STAT5b staining, score 2 with 25-50%, score 3 with 50-75% and score 4 with 75-100%). Clinical data of the patients were retrieved form the charts of the patients, following ethical and IRB approval at the UMC Utrecht (approval nos. 16-229 and 16-342) and are provided in Table SI. Preoperative MRI scans available for 167 of the first 196 patients of our institutional cohort were analyzed by a trained radiologist for the following signs of tumor dissemination: the presence (or not) of tumor islets at a distance of the tumor mass, a ratio >2 between the maximal diameters of the T2-weighted extent of the tumor and of the contrast-enhancing T1-weighted tumor area, and the invasion of the corpus callosum by the enhancing component of the tumor.

Cell cultures, reagents and small interfering (si)RNA. The genetic profile of human LN18 GBM (cat. no. CRL-2610; ATCC) and U87 malignant glioma cells of unknown origin (cat. no. HTB-14; ATCC) was verified using CGH (Affymetrix SNP6.0 arrays) and TP53 sequencing (ion torrent). GM2 and GM3 primary GBM cells were derived from fresh samples of human GBM and cultured as previously described (20). They were characterized using GFAP IHC, TP53, IDH1/2 (both wild-type), and $EGFR_{VIII}$ (both negative) mRNA sequencing and by CGH analysis, and maintained at low passages. $U87_{VIII}$ cells were kindly provided by Dr M. Broekman (University Medical Center of Utrecht) and their expression of $EGFR_{VIII}$ was confirmed by next generation sequencing. Cells were cultured in 5% CO_2 in DMEM (Thermo Fisher Scientific, Inc.) supplemented with 10% FBS (Gibco; Thermo Fisher Scientific, Inc.) and 1% of 5 mg/ml penicillin-streptomycin (Gibco; Thermo Fisher Scientific, Inc.) solution at 37˚C, and maintained at low passages.

For siRNA experiments, 70% confluent cultured cells were transiently transfected with 25 nM of Control pool non-targeting #1 (D-001810-10-05) or SMARTpool human STAT5b siRNA (M-010539-02) from Dharmacon using the DharmaFECT transfection reagent (Thermo Fisher Scientific, Inc.; DharmaFECT Transfection Reagents) according to the manufacturer's protocol at 37˚C. Transfection time was 48 h, after which the cells were used for subsequent experimentations.

Western blot analysis. Whole-cell lysate were obtained using lysis SDS 1% buffer containing protease and phosphatase inhibitors. Protein concentration was determined using BCA method (Pierce kit; Thermo Fisher Scientific, Inc.), and 25 μg of protein were loaded per lane. Western blot analysis was performed in polyacrylamide 10% gels and run for 1 h and 30 min at 100 V, then transferred to PVDF membrane (Roche Diagnostics) for 1 h at 100 V. Blocking was performed for 1 h at room temperature, in the same buffers used for the incubation of the respective antibodies. All primary antibodies were incubated overnight at 4˚C and the dilution recommended by the manufacturer was used; STAT5b (Abcam; cat. no. ab194380; 1:5,000 in 4% BSA (VWR International, LLC), 1X TBS, 0.1% Tween® 20 buffer), GAPDH (Sigma-Aldrich; Merck KGaA; cat. no. PLA0125; 1:10,000 in 4% non-fat dry milk, 1X TBS, 0.1% Tween® 20), p27 (Cell Signaling Technology, Inc.; cat. no. 3688; 1:1,000 in 4% BSA 1X TBS, 0.1% Tween® 20 buffer),

Cyclin D1 (Cell Signaling Technology, Inc.; cat. no. 2922; 1:1,000 in 4% BSA 1X TBS, 0.1% Tween®-20 buffer), BCL-XL (Cell Signaling Technology, Inc.; cat. no. 2764; 1:1,000 in 4% BSA 1X TBS, 0.1% Tween®-20 buffer) and PD-L1 (Cell Signaling Technology, Inc.; cat. no. 13684; 1:1,000 in 4% BSA 1X TBS, 0.1% Tween®-20 buffer). Appropriate HRP-linked secondary antibody was used (Cell Signaling Technology, Inc.; cat. no. 7074; 1:3,000) for incubation at room temperature during 2 h with gentle shaking. For detection, enhanced chemiluminescence method was used. Clarity Western ECL Blotting Substrate (Bio-Rad Laboratories, Inc.) was used coupled with film-based imaging following the manufacturer's protocol.

Cell survival assays. After 24 h of transfection, 2,500 cells were seeded in 96-well plate, then let to adhere overnight before to support Temozolomide (TMZ; cat. no. T2577; Sigma-Aldrich; Merck KGaA) treatment or gamma-radiation and later MTS assay (One solution cell proliferation assay; cat. no. G3582; Promega Corporation) as recommended by the manufacturer, and the absorbance was measured at 490 nm.

Clonogenic assays. After 48 h of siRNA transfection, 500 cells were seeded in six-well plate followed or not with gamma-radiation, then left to grow for 7 days and then fixed in 4% paraformaldehyde (45 min at room temperature) and stained with crystal violet (5 mg/ml) for 10 min at room temperature before counting on a light microscope (Olympus Corporation).

Migration/Invasion assays. For Boyden chamber assays, 48 h post-siRNA transfection, a calculated number of cells (50,000 for U87, GM2 and GM3; 25,000 for U87VIII and LN18) in serum-free medium with 0,1% BSA (VWR International, LLC) were seeded into the upper chamber of Transwell inserts (8 μm) coated with collagen type I (50 μg/ml) for migration and with Matrigel (500 μg/ml; precoating for 30 min at 37˚C) for invasion, whereas medium with 1,5% FBS and 1% BSA was applied in the lower chamber as chemo-attractant. After 6 h of migration or 24 h of invasion, cells were fixed with 4% paraformaldehyde and stained with 0.4% crystal violet (ambiant temperature, 10 min), scanned on a Hamamatsu NDP scanner, and counted. For wound healing (scratch) assays, 48 h post-siRNA transfection cells were cultured until confluence and treated for 1 h with mitomycin C (Sigma-Aldrich; Merck KGaA) and then wounded using a 100-μl pipette tip. Images of the migration distance were captured on a phase contrast Leica microscope and measured at zero time and after 1, 4, 6, 20 and 24 h and expressed in percentages of the original gap. For quantification, the margins were plotted and 3 measurements were made per scratch, and averaged to calculate the healing percentage. Each condition was performed in quadruplicate.

Statistical analysis. Statistical analysis was performed using the Prism 5.0 (GraphPad Software, Inc.) and the SPSS 24 (IBM Corp.) software. Kaplan-Meier survival estimates were obtained and multivariable Cox regression analysis was performed taking the age, KPS (> or <70), tumor volume (in cubic cm, measured with Osirix® and based on the contrast-enhancing T1-weighted tumor boundaries), type of surgery (biopsy vs. debulking) and IDH R132H status into account to assess correlation with overall survival. Survival data were censored at 1,000 days in order to comply with the condition of proportional hazard for the survival analyses (19). Multiple t-tests and two-way ANOVA, with Dunnett's multiple comparisons post hoc tests were performed as appropriate for non-survival data. Correlations were assessed using Pearson's test. The association of low or high Stat5b activation with MRI criteria of invasion was assessed by Chi-square and Kruskall Wallis tests. Results are expressed as the mean ± SD and a two-sided $P<0.05$ was considered to indicate a statistically significant difference.

Results

STAT5b activation and GBM patient survival. Agilent-based STAT5b mRNA expression values and gene copy number (CN) were obtained for 552 patients of the TCGA repository of GBM. There was a weak correlation between the mRNA expression of STAT5b and its copy number (Pearson's correlation 0.091, $P=0.033$), but this CN did not correlate with patient survival (data not shown). Similarly, the mRNA expression of STAT5b mRNA did not correlate with patient survival in a Cox survival model taking the Karnofsky performance score (KPS) and patient age into account ($P=0.696$). TMAs were obtained for a series of 392 patients treated at our neuro-oncological center and for 10 non-tumor brain tissue samples obtained from temporal lobe epilepsy surgery.

IHC showed a high level of nuclear expression of Phospho-STAT5b (p-STAT5b) in a majority of the samples, including in the non-tumor brain samples. In these non-tumor samples, 75% of non-neuronal cells presented a positive staining of the nucleus for STAT5b, i.e., an immunochemistry score of 3 (Fig. S1). In the GBM patients, there was an inverse correlation between the nuclear staining score for nuclear p-STAT5b (taken as a continuous variable) and overall survival in a multivariable Cox model taking the Age, KPS, tumor volume, type of surgery and IDH1R132 mutational status into account [hazard ratio (HR), 1.22; 95% confidence interval (CI), 1.111-1.346; $P<0.001$]. Also significant in this analysis were the patient age and KPS (Table SII for). This multivariable analysis remained even significant when the patients were dichotomized between two groups based on a practical threshold of 3, corresponding to that of 'non-tumor' p-STAT5b nuclear staining instead of a continuous variable (HR 1.664; 95% CI 1.290-2.150; $P<0.001$; Table I). Kaplan Meier survival estimates based on this threshold showed a median survival of 13.5 months in the low STAT5b activation group vs. only 9.3 months in the high STAT5b activation group of patients ($P<0.001$, Log Rank test, Fig. 1).

STAT5b and GBM cell proliferation. Transfection of human GBM cell cultures using a SMARTpool® of human STAT5b siRNA resulted in a significant and lasting STAT5b protein knockdown (80% protein reduction minimum) within 24 h (Fig. 2A). This depletion of STAT5b did not prove cytotoxic to any of the GBM cells as measured by a MTS test for 72 h (NS, ANOVA, n=3, Fig. 2B). In clonogenic assays, STAT5b knockdown even induced a slight but significant increase in

Table I. Multivariate Cox regression analysis of the overall survival of 392 glioblastomapatients form our institutional cohort.

			95% CI for HR	
Variables in the Cox model	P-value	HR	Lower	Upper
Nuclear p-STAT5b IHC score (>3 vs. <3)	<0.001	1.664	1.290	2.150
Age at diagnosis	<0.001	1.037	1.024	1.05
KPS (<70 vs. >70)	<0.001	2.387	1.811	3.147
Type of surgery (Biopsy vs. debulking)	0.191	1.349	0.862	2.111
IDH1 R132H gene (wild-type vs. mutant)	0.06	2.207	0.967	5.037

KPS, Karnofsky Performance Scale score; CI, confidence interval; HR, hazard ratio.

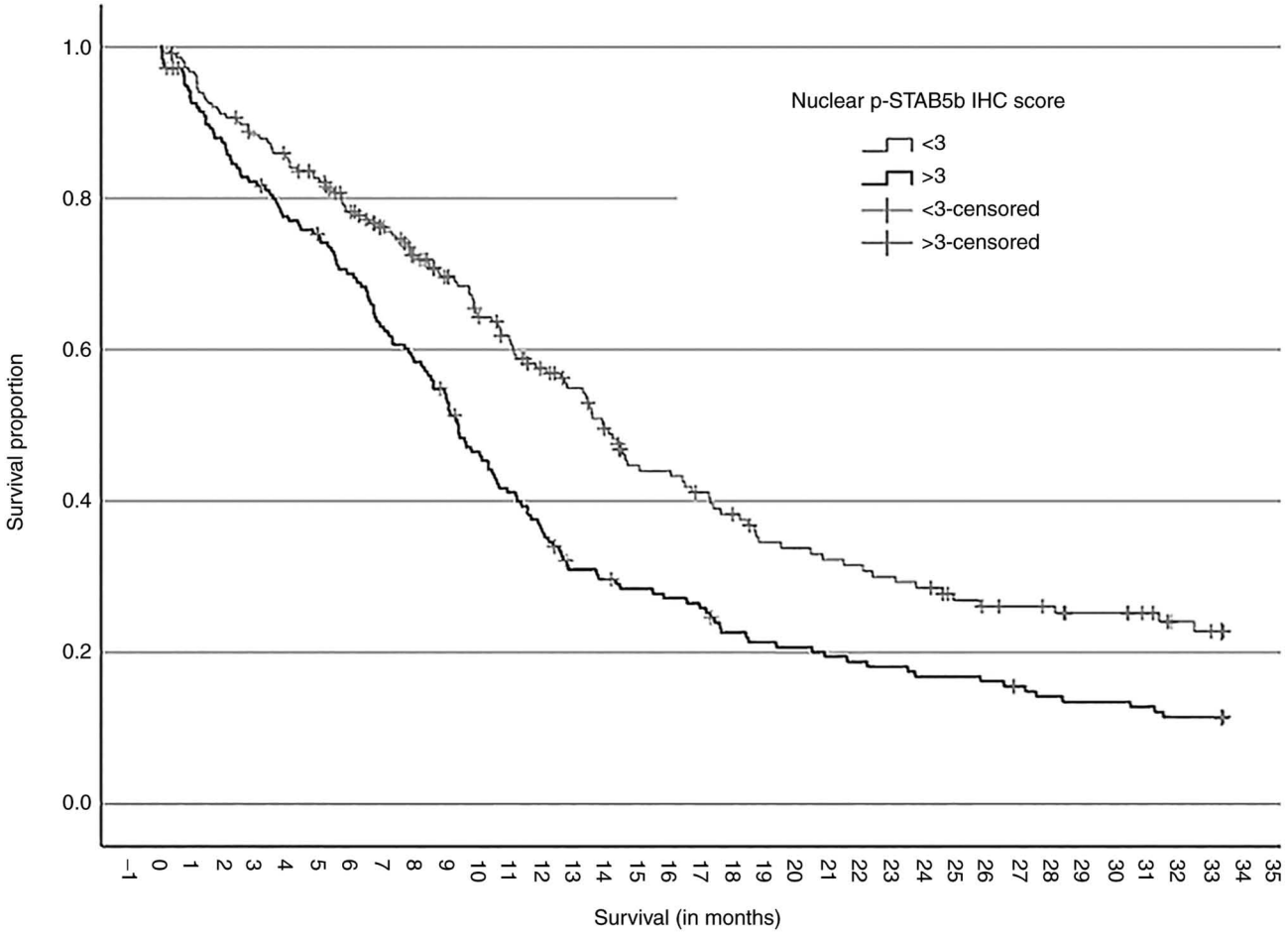

Figure 1. STAT5b expression in human GBM and patient survival. Kaplan-Meier overall survival curves for low GBM STAT5b expression (score <3) and high GBM STAT5b expression (score ≥3) in a population of 392 GBM patients. P<0.001, Log Rank test. Examples of corresponding histological slides are provided in Fig. S1. GBM, glioblastoma.

colony (minimum 20 cells) formation in U87 and GM3 cells (P<0.01; n=3, Fig. 2C), and did not alter that of $U87_{VIII}$, LN18 and GM2 cells. STAT5b depletion also resulted in a reproducible decrease of the cell cycle inhibitor $p27^{kipl}$ (Fig. 2D) and a reproducible increase of Cyclin D1 in all cell types (Fig. 2E). In search for additional effects, STAT5b inhibition did not affect expression the expression of Bcl-XL (Fig. S4), on GBM cells, and increased the expression of the immune checkpoint ligand PD-L1 (Fig. S5) in these cells.

STAT5b and chemo/radio-sensitivity of GBM cells. Given the inverse correlation between p-STAT5b nuclear expression and survival in our cohort of GBM patients and a previous study that STAT5b contributes to chemoresistance of of GBM to cisplatin (12), it was investigated whether this transcription factor would also contribute to the resistance of these tumors to their conventional treatments, namely ionizing radiation and TMZ chemotherapy. In clonogenic assays performed with increasing doses of radiation (0-2-4 Gy), STAT5b knockdown

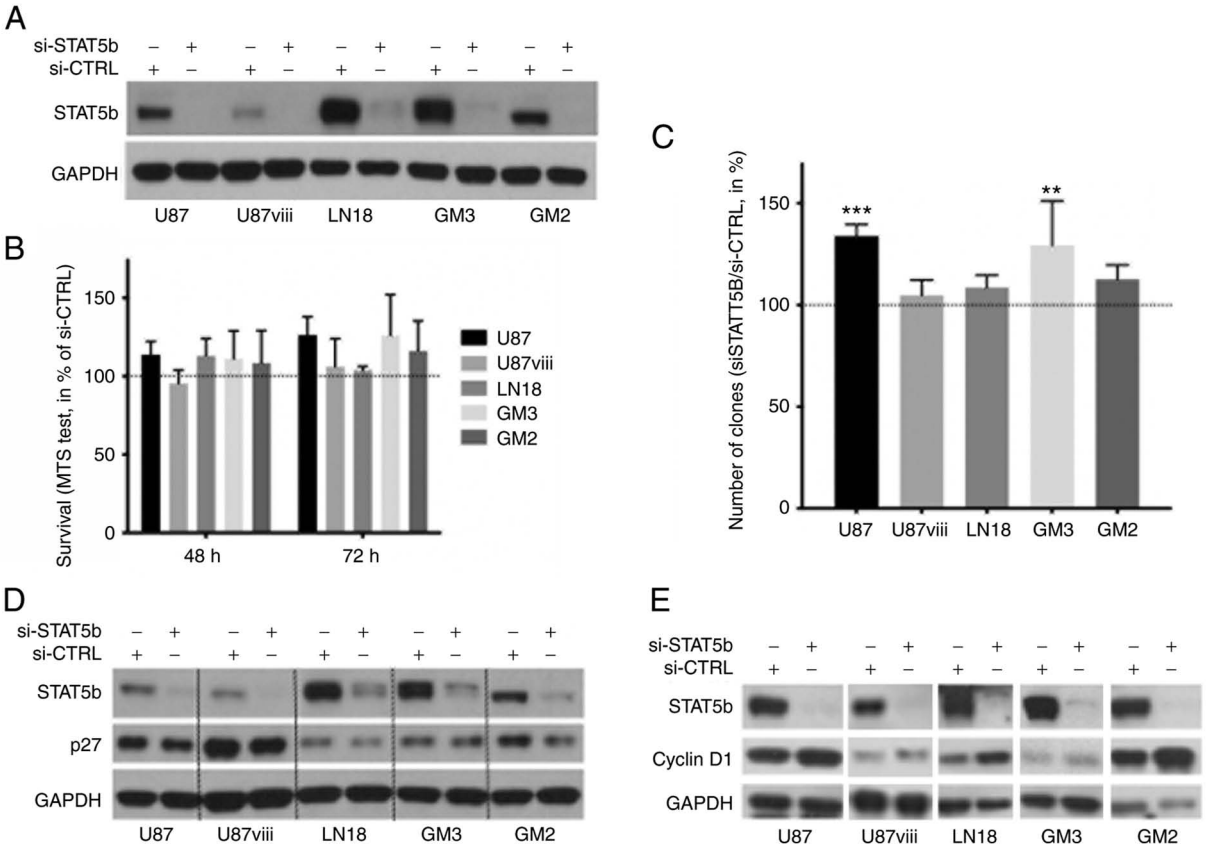

Figure 2. STAT5b knockdown and glioblastoma proliferation capacities. (A) STAT5b protein level expression after 48 h of siRNA transfection evaluated by western blot analysis. (B) Survival MTS assay after siSTAT5b transfection, survival expressed in percentage of siControl. (C) Colony forming after transient siSTAT5b transfection, surviving fraction expressed in percentage of the siControl number of colonies. (D and E) $p27^{Kipl}$ and Cyclin D1 protein level expression after 24 and 48 h post-siRNA transfection, respectively. The densitometric measurements of the different western blots are provided in Table SIII. Data are shown as the mean ± SD. **P<0.01 and ***P<0.001. si-, small interfering.

did not affect the radiation sensitivity of U87 and U87viii cells. STAT5b depletion even slightly but significantly protected LN18, GM3 and GM2 cells against radiation toxicity (P<0,01, two-ways ANOVA, n=4, Fig. 3A). The sensitivity of GBM cells to TMZ treatment (800 μM) was not significantly affected by STAT5b depletion (Fig. 3B).

STAT5b and GBM dissemination. In scratch assays, the closure kinetic of the monolayer gap was assessed for 24 h, and was similar between siSTAT5b and siControl in both U87 and $U87_{VIII}$ cells. The healing was however slightly faster in siSTAT5b-than in siControl-treated LN18 cells, lasting 20 vs. 24 h. Similarly, siSTAT5b-treated GM3 and GM2 cells healed significantly faster than their siControl counterparts (Figs. 4A and S2). Following STAT5b knockdown, the migration of U87, LN18 and GM2 cells through collagen-coated membranes of Boyden chambers increased significantly as well (by 197,7±65,4%, 201,6±11,2% and 219,7±21% respectively; P<0,001; n=3), while that of $U87_{VIII}$ and GM3 remained unaffected [Fig. 4B (a) and (b)].

When the Boyden membranes were coated with Matrigel however, the invasion of $U87_{VIII}$, GM3 and GM2 cells decreased by 53,2±17,1%, 52,2±11,9% and 43,5±15,6% upon STAT5b depletion (P<0,0001; n=4 for GM3 and n=5 for $U87_{VIII}$ and GM2; Figs. 4C and S3), while that of U87 and LN18 did not change significantly.

Finally, in order to assess the resulting clinical effect of these diverging effects of STAT5b on migration and invasion of GBM, the available T1-weighted, gadolinium-enhanced MRI images of the first half of our patients (available in 167/196 patients) were analyzed for signs of tumor dissemination. The presence (or not) of tumor islets at a distance of the tumor mass, a ratio >2 between the maximal diameters of the T2-weighted extent of the tumor and of the contrast-enhancing T1-weighted tumor area, or invasion of the corpus callosum by the enhancing component of the tumor were assessed. There was neither any difference between the level of nuclear STAT5b staining between tumors presenting either of these dissemination features or not (N.S., Kruskall-Wallis non-parametric test), nor was there any association between a high STAT5b IHC score (>3) and these parameters (N.S., Chi-square test).

Discussion

STAT5a and STAT5b present overlapping and distinct regulatory pathways and transcriptional targets (5,8), and while STAT5a has been shown to favor the proliferation of malignant gliomas, STAT5b appears to be predominantly activated in GBM (7,14) and has been proposed as a therapeutic target against these tumors (16).

As previously described, indeed (6,7,17), GBM from our cohort revealed a high level of STAT5b activation. This activation was often higher than that of the glial cells

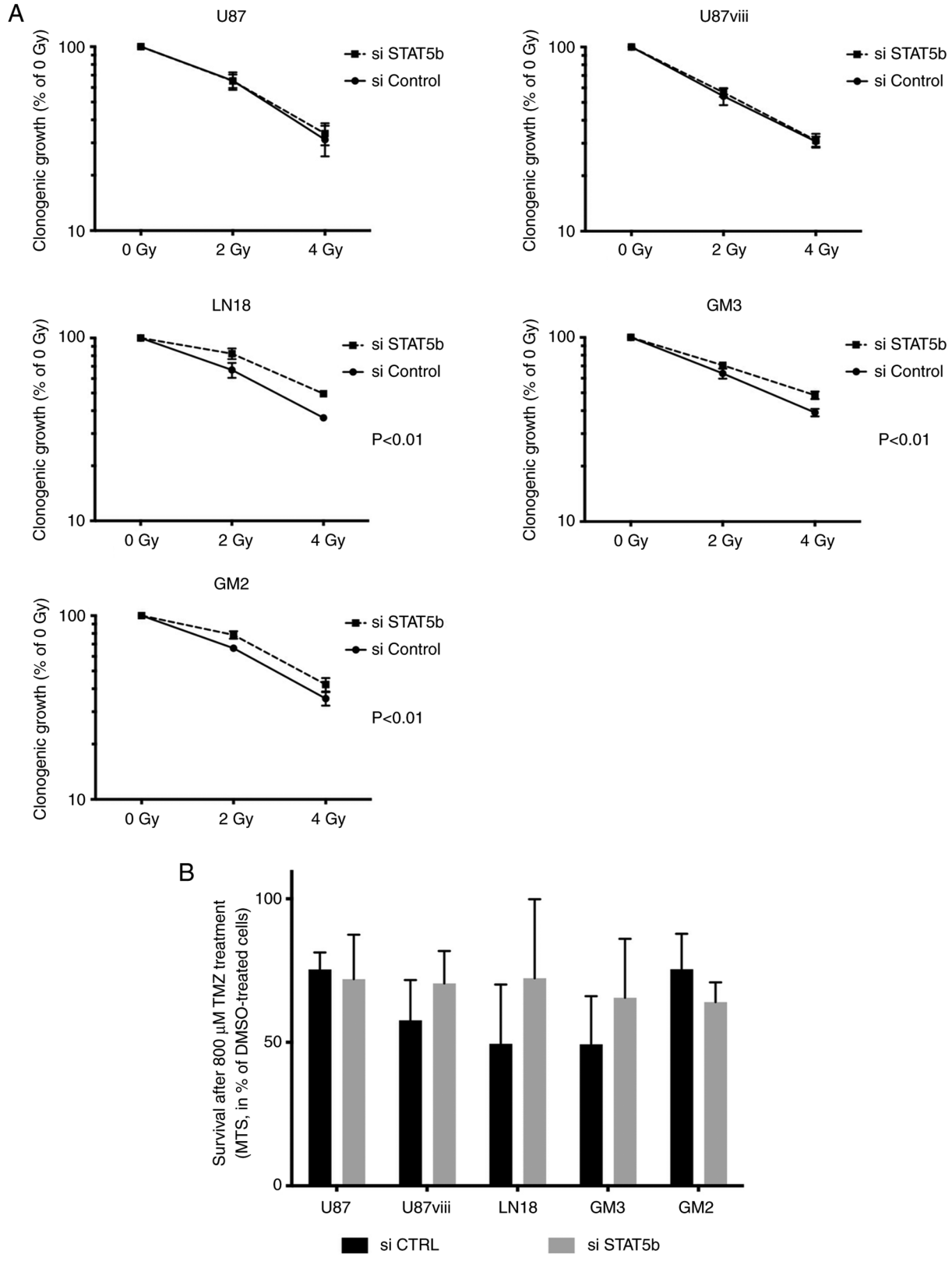

Figure 3. STAT5b knockdown and radiation or chemo-sensitivity of GBM cells. (A) Clonogenic assays of GBM cells transfected with siSTAT5b or siControl followed by gamma-radiation (0, 2 or 4 Gy). The number of growing colonies after 7 days is expressed in percentage as compared with unirradiated cells (0 Gy). (B) MTS survival assay performed after 800 μM temozolomide treatment on cells transfected with siSTAT5b or siControl, survival expressed in percentage of siControl transfected cells. Data are presented as the mean ± SD, n=3. GBM, glioblastoma; si-, small interfering.

of non-tumoral brain samples, and is inversely correlated with patient survival. The present Kaplan-Meier estimates demonstrated that tumors with a high level of nuclear p-STAT5b staining had a median overall survival more than 4 months shorter than those with a low STAT5b activation level. This prognostic association remains highly significant

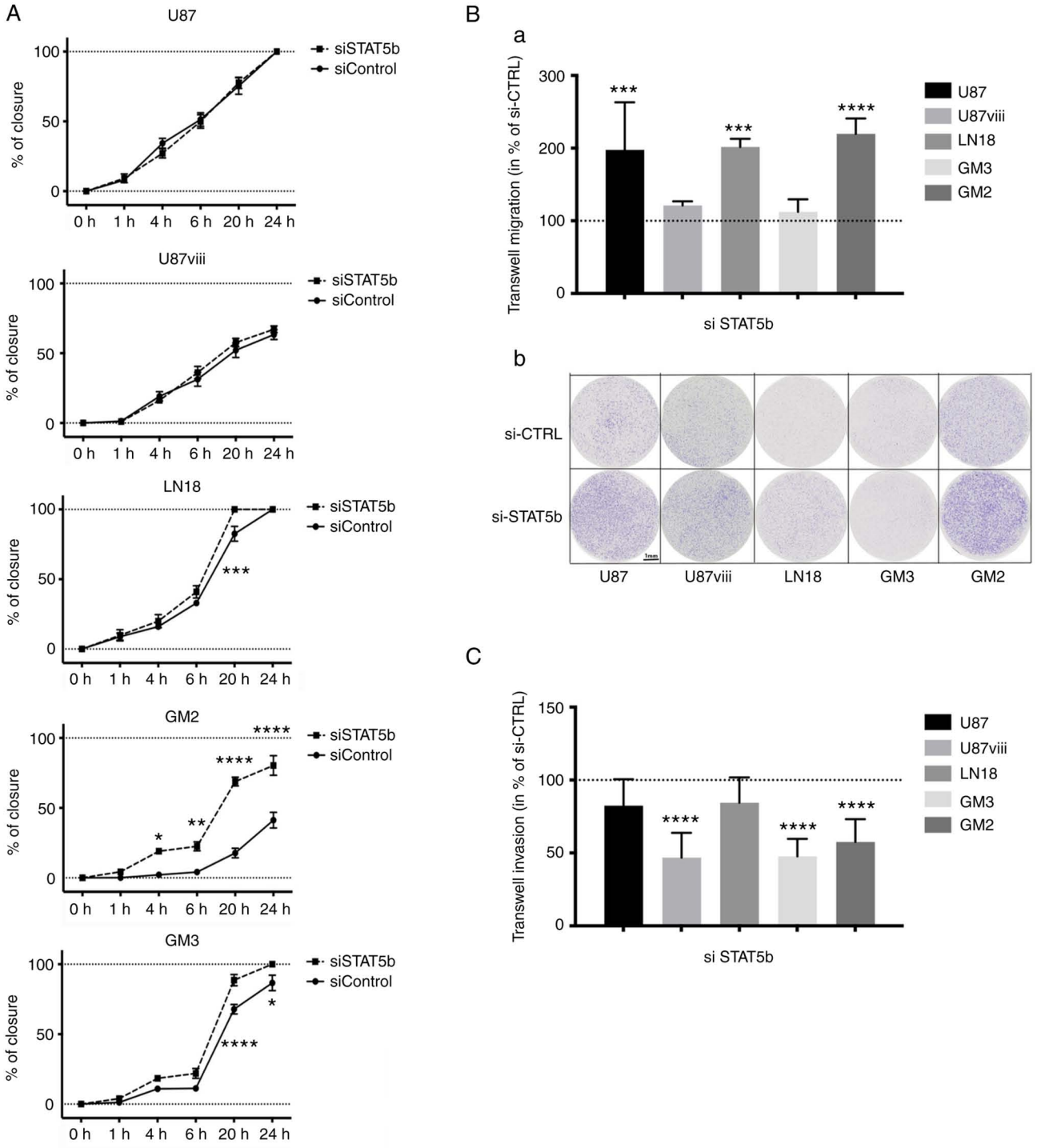

Figure 4. STAT5b and tumor invasion. (A) Wound healing assay after STAT5b inhibition, distance represented as percentage of wound closure. (B) (a) Transwell migration assay performed 48 h after siRNA transfection, migration expressed in percentage of siControl transfected cells after 6 h of migration; (b) representative pictures of the migration experiments. (C) Matrigel-coated Transwell invasion assay performed 48 h post-transfection. Invasion expressed in percentage of siControl transfected cells after 24 h of invasion. Data are presented as the mean ± SD, n=8 for each condition. *P<0.05, **P<0.01, ***P<0.001 and ****P<0.0001. si-, small interfering.

in multivariable analysis independent of the KPS, age, tumor volume, type of surgery or IDH1 R132H mutation. The present findings confirmed and extented those of previous survival analyses that were performed in monovariable fashion and on much smaller cohorts of patients (6,17). It was also observed that neither the copy number nor the mRNA expression of STAT5b correlated with survival in GBM patients, suggesting that it is truly the nuclear activation of STAT5b, rather than its mere expression, that correlates with the prognosis of patients with a GBM.

Despite its inverse association with patient survival, STAT5b activation did not support GBM cell proliferation. On the contrary in fact, the inhibition of STAT5b reduced the expression of p27 and increased that of Cyclin D1 in our panel of cell lines and primary cultures of GBM, and even slightly increased the clonogenic potential of U87 and

GM3 cells. This contrasts with the proliferative actions of STAT5a (12,13), and likely underscores the specificity of these two STAT family members (10). Notably, Liang *et al* (7) observed that a less complete depletion of STAT5b than in our experiments decreased the proliferation of some GBM cell lines. This suggested that the effects of STAT5b could be concentration-dependent and non-linear, or could depend on a more complex balance with other transcription factors. It was also noted that the pro-clonogenic effect of STAT5b knockdown observed in U87 cells, was absent in $U87_{vIII}$ cells. $EGFR_{vIII}$ has been identified to form nuclear STAT5b-$EGFR_{vIII}$ complexes in GBM (8,21), which activate BCL_{XL} and favor cell survival (8,22), and could have contributed this difference. However, no alteration of Bcl-XL expression was observed in our experimental conditions following STAT5b knockdown, and other cell-specific mechanisms must be at play. Altogether, and most importantly, the effects of STAT5b on the proliferation of malignant gliomas remain variable from tumor to tumor, and this should caution the targeting of STAT5b for therapeutic goals.

In line with a previous study (9), it was observed that the invasion of several GBM cell cultures decreased upon STAT5b inhibition. However, and in contrast with a previous study (7), STAT5b inhibition increased the migration of most of our GBM cells in wound healing and Transwell migration experiments. Differential effects of a given signaling pathways are uncommon, but have been observed previously, notably for the focal adhesion kinase FAK, a target of STAT5 signaling (7,23). As a likely result of these opposite effects of STAT5b on invasion and migration, no correlation was found between STAT5b activation and tumor invasion on the MRI scans of our patients.

STAT5b has also been revealed to protect GBM cells against the cytotoxic effects of DNA-damaging agents such as cisplatin (8). However, no sensitization of GBM cells to TMZ or ionizing radiations was observed following STAT5b inhibition, and even a slight protection against these conventional anti-GBM cytotoxic agents was identified in some of the cultures of the present study. Finally, it was revealed that STAT5b inhibition also increased the expression of the immune checkpoint ligand PD-L1 on GBM cells, further casting doubts on the potential of STAT5b as a potential therapeutic target in GBM.

Collectively, the present findings clearly defined the potential of activated nuclear p-STAT5b as a prognostic marker of patient survival in GBM, independent on IDH1 R132H status and other classical predictors of longevity. Given its lack of significant proper oncogenic role however, our results do not support anti-STAT5b strategies as a means to treat GBM. Rather, nuclear p-STAT5b appears to be a surrogate marker of the activation of true oncogenic pathways, possibly HIF-1α (18) or tyrosine kinase receptors, which are frequently hyper-activated in GBM (8,11,24) and can, besides the JAK/STAT cascade, activate known oncogenic pathways such as the ERK/MAP kinases or the NF-kappaB pathways (3,14,20,25).

Acknowledgements

The authors would like to thank Dr J. Hendrikse (UMC Utrecht) for his help assessing the MRI criteria of invasion.

Funding

The present study was supported by Televie grants (grant nos. 1.7.247.330.12 and 7.4567.15) from the FNRS of Belgium, the Belgian National Cancer Plan (grant no. 20-044) and the T&P Bohnenn Fund for Neuro-Oncology research.

Availability of data and materials

The datasets used and/or analyzed during the current study are available from the corresponding author on reasonable request.

Authors' contributions

Conceptualized the study. ND and PAR wrote the prepared and wrote the draft. ND and PAR revised and edited the manuscript. ND, TS, LS, KT, SB, WS and PAR performed data acquisition, experiments and analysis. PAR and VB supervised the study. PR, VB and TS acquired funding. All authors read and approved the final manuscript. PAR, VB and ND confirm the authenticity of all the raw data.

Ethics approval and consent to participate

The present study was conducted following review by the local ethical committee and the institutional review board (TC-Bio; approval nos. 16-229 and 16-342). According to Dutch regulations, the need for informed consent was waived for this retrospective analysis of patient clinical data.

Patient consent for publication

Not applicable.

Competing interests

The authors declare that they have no competing interests.

References

1. Stupp R, Mason WP, van den Bent MJ, Weller M, Fisher B, Taphoorn MJ, Belanger K, Brandes AA, Marosi C, Bogdahn U, *et al*: Radiotherapy plus concomitant and adjuvant temozolomide for glioblastoma. N Engl J Med 352: 987-996, 2005.
2. Stupp R, Taillibert S, Kanner AA, Kesari S, Steinberg DM, Toms SA, Taylor LP, Lieberman F, Silvani A, Fink KL, *et al*: Maintenance therapy with tumor-treating fields plus temozolomide vs temozolomide alone for glioblastoma: A randomized clinical trial. JAMA 314: 2535-2543, 2015.
3. Bell EH, Pugh SL, McElroy JP, Gilbert MR, Mehta M, Klimowicz AC, Magliocco A, Bredel M, Robe P, Grosu AL, *et al*: Molecular-based recursive partitioning analysis model for glioblastoma in the temozolomide era: A correlative analysis based on NRG oncology RTOG 0525. JAMA Oncol 3: 784-792, 2017.
4. Eckel-Passow JE, Lachance DH, Molinaro AM, Walsh KM, Decker PA, Sicotte H, Pekmezci M, Rice T, Kosel ML, Smirnov IV, *et al*: Glioma groups based on 1p/19q, IDH, and TERT promoter mutations in tumors. N Engl J Med 372: 2499-2508, 2015.
5. Maurer B, Kollmann S, Pickem J, Hoelbl-Kovacic A and Sexl V: STAT5A and STAT5B-twins with different personalities in hematopoiesis and leukemia. Cancers (Basel) 11: 1726, 2019.
6. Kuo YH, Chen YT, Tsai HP, Chai CY and Kwan AL: Nucleophosmin overexpression is associated with poor survival in astrocytoma. APMIS 123: 515-522, 2015.

7. Liang QC, Xiong H, Zhao ZW, Jia D, Li WX, Qin HZ, Deng JP, Gao L, Zhang H and Gao GD: Inhibition of transcription factor STAT5b suppresses proliferation, induces G1 cell cycle arrest and reduces tumor cell invasion in human glioblastoma multiforme cells. Cancer Lett 273: 164-171, 2009.
8. Latha K, Li M, Chumbalkar V, Gururaj A, Hwang Y, Dakeng S, Sawaya R, Aldape K, Cavenee WK, Bogler O and Furnari FB: Nuclear EGFRvIII-STAT5b complex contributes to glioblastoma cell survival by direct activation of the Bcl-XL promoter. Int J Cancer 132: 509-520, 2013.
9. Cao S, Wang C, Zheng Q, Qiao Y, Xu K, Jiang T and Wu A: STAT5 regulates glioma cell invasion by pathways dependent and independent of STAT5 DNA binding. Neurosci Lett 487: 228-233, 2011.
10. Lin JX and Leonard WJ: The role of Stat5a and Stat5b in signaling by IL-2 family cytokines. Oncogene 19: 2566-2576, 2000.
11. Chumbalkar V, Latha K, Hwang Y, Maywald R, Hawley L, Sawaya R, Diao L, Baggerly K, Cavenee WK, Furnari FB and Bogler O: Analysis of phosphotyrosine signaling in glioblastoma identifies STAT5 as a novel downstream target of ΔEGFR. J Proteome Res 10: 1343-1352, 2011.
12. Roos A, Dhruv HD, Peng S, Tuncali S, Pineda M, Millard N, Mayo Z, Eschbacher JM, Loftus JC, Winkles JA and Tran NL: EGFRvIII-Stat5 signaling enhances glioblastoma cell migration and survival. Mol Cancer Res 16: 1185-1195, 2018.
13. Tan C, Dai Y, Liu X, Zhao G, Wang W, Li J and Qi L: STAT5A induced LINC01198 promotes proliferation of glioma cells through stabilizing DGCR8. Aging (Albany NY) 12: 5675-5692, 2020.
14. Zhang Y, Kim J, Mueller AC, Dey B, Yang Y, Lee DH, Hachmann J, Finderle S, Park DM, Christensen J, *et al*: Multiple receptor tyrosine kinases converge on microRNA-134 to control KRAS, STAT5B, and glioblastoma. Cell Death Differ 21: 720-734, 2014.
15. Sawada T, Arai D, Jing X, Miyajima M, Frank SJ and Sakaguchi K: Molecular interactions of EphA4, growth hormone receptor, Janus kinase 2, and signal transducer and activator of transcription 5B. PLoS One 12: e0180785, 2017.
16. Liu YL, Liu PF, Liu HE, Ma LX and Li G: Association between STAT5 polymorphisms and glioblastoma risk in Han Chinese population. Pathol Res Pract 210: 582-585, 2014.
17. Televantou D, Karkavelas G, Hytiroglou P, Lampaki S, Iliadis G, Selviaridis P, Polyzoidis KS, Fountzilas G and Kotoula V: DARPP32, STAT5 and STAT3 mRNA expression ratios in glioblastomas are associated with patient outcome. Pathol Oncol Res 19: 329-343, 2013.
18. Berendsen S, Spliet WGM, Geurts M, Van Hecke W, Seute T, Snijders TJ, Bours V, Bell EH, Chakravarti A and Robe PA: Epilepsy associates with decreased HIF-1α/STAT5b signaling in glioblastoma. Cancers (Basel) 11: 41, 2019.
19. Berendsen S, Varkila M, Kroonen J, Seute T, Snijders TJ, Kauw F, Spliet WG, Willems M, Poulet C, Broekman ML, *et al*: Prognostic relevance of epilepsy at presentation in glioblastoma patients. Neuro Oncol 18: 700-706, 2016.
20. Robe PA, Bentires-Alj M, Bonif M, Rogister B, Deprez M, Haddada H, Khac MT, Jolois O, Erkmen K, Merville MP, *et al*: In vitro and in vivo activity of the nuclear factor-kappaB inhibitor sulfasalazine in human glioblastomas. Clin Cancer Res 10: 5595-5603, 2004.
21. Fan QW, Cheng CK, Gustafson WC, Charron E, Zipper P, Wong RA, Chen J, Lau J, Knobbe-Thomsen C, Weller M, *et al*: EGFR phosphorylates tumor-derived EGFRvIII driving STAT3/5 and progression in glioblastoma. Cancer Cell 24: 438-449, 2013.
22. Yang C, Huang W, Yan L, Wang Y, Wang W, Liu D and Zuo X: Downregulation of the expression of B-cell lymphoma-extra large by RNA interference induces apoptosis and enhances the radiosensitivity of nonsmall cell lung cancer cells. Mol Med Rep 12: 449-455, 2015.
23. Hsia DA, Mitra SK, Hauck CR, Streblow DN, Nelson JA, Ilic D, Huang S, Li E, Nemerow GR, Leng J, *et al*: Differential regulation of cell motility and invasion by FAK. J Cell Biol 160: 753-767, 2003.
24. Gressot LV, Doucette TA, Yang Y, Fuller GN, Heimberger AB, Bögler O, Rao A, Latha K and Rao G: Signal transducer and activator of transcription 5b drives malignant progression in a PDGFB-dependent proneural glioma model by suppressing apoptosis. Int J Cancer 136: 2047-2054, 2015.
25. Bredel M, Scholtens DM, Yadav AK, Alvarez AA, Renfrow JJ, Chandler JP, Yu IL, Carro MS, Dai F, Tagge MJ, *et al*: NFKBIA deletion in glioblastomas. N Engl J Med 364: 627-637, 2011.